Journal of Pipeline Science and Engineering 3 (2023) 100128

Contents lists available at ScienceDirect

Journal of Pipeline Science and Engineering

journal homepage: http://www.keaipublishing.com/en/journals/journal-of-pipeline-science-and-engineering/

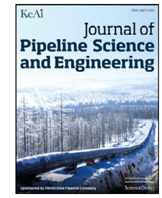

Terzaghi's three stability factors for pipeline burst-related ground stability

Jim Shiau[a], Suraparb Keawsawasvong[b,*], Rungkhun Banyong[b]

[a] School of Engineering, University of Southern Queensland, Toowoomba, QLD, Australia
[b] Research Unit in Sciences and Innovative Technologies for Civil Engineering Infrastructures, Department of Civil Engineering, Thammasat School of Engineering, Thammasat University, Pathumthani 12120, Thailand

ARTICLE INFO

Keywords:
Water mains
Blowout
Stability
Trapdoor
Limit analysis

ABSTRACT

A recent study on active trapdoor stability has been completed by the authors using Terzaghi's three stability factors approach. It was concluded that the superposition approach is an effective way to evaluate the stability of cohesive-frictional soils. This technical note aims to extend the previous active trapdoor study to perform a stability assessment of a passive planar trapdoor (i.e., a blowout condition) in cohesive-frictional soil. Note that this passive trapdoor problem represents the blowout stability of soils due to defective pipelines under high water main pressures, in spite of the frequent media news about the water main bursts which enlightens the relevance of the problem. Numerical solutions of upper and lower bound finite element limit analyses are presented in form of the three stability factors (F_c, F_s, *and* F_γ), which consider the effect of cohesion, surcharge, and soil unit weight respectively. In the event of passive trapdoor stability, this technique can be used to determine a critical blowout pressure due to a water mains leak. The study continues with a series of sensitivity analyses with a widely selected range of parameters including the cover-depth ratio (H/B) and the drained frictional angle (ϕ). The influence of these parameters on the three stability factors is discussed, and a practical example of adapting these approaches is also introduced. All numerical results are provided in the forms of design charts and tables that can be efficiently used with confidence in design practice.

1. Introduction

Population increases and the growth in urban regions demand an effective utilization of infrastructures in the modern world. To meet the demands, the construction of public utilities have grown significantly, particularly in underground water pipeline systems. From a geotechnical stability point of view, underground water mains blowout can be represented by the classical trapdoor problem with an uplift mechanism where the internal water pressure is greater than the soil shear resistance as well as the soil self-weight. A significant number of research on the stability of trapdoors have been published since the pioneering work of Terzaghi (1936), who classified soil collapse as either active failure due to the action of soil self-weight and surface surcharge or passive failure occurring as a result of an elevating force against the direction of soil movement due to gravity.

In its theoretical form, the blowout stability is like a ground anchor subjected to uplift force resulting in a passive failure mechanism. Meyerhof and Adams (1968), Kupferman (1965), Vesic (1971), Meyerhof (1973), Das (1978, 1980), and Das et al. (1994) are among the researchers who investigated the uplift capability of embedded anchors in soils through experiment testing. For the passive trapdoor, Vardoulakis et al. (1981) conducted a series of physical tests in cohesionless sands, establishing analytical solutions for both passive and active trapdoors. The passive scenario was represented by a wedge extending outwards from a certain trapdoor to the ground free surface, but the active wedge at the ultimate limit state was regarded as a vertical mechanism as suggested by Terzaghi (1946).

Regarding works of numerical simulations, Koutsabeloulis and Griffiths (1989) conducted a series of Finite Element (FE) studies for active and passive trapdoors in soils. Smith (1998) demonstrated a computational approach for solving trapdoor load ratios in cohesionless soils employing the Discontinuity Layout Optimization (DLO) algorithm as well as an Upper Bound (UB) limit analysis. Moreover, by employing a set of dimensionless charts with upper bound analysis. Martin (2009) further investigated the failure mechanism and collapse load of the undrained active and passive trapdoor through upper bound and lower bound approaches by utilizing the novel slip line method to determine the actual collapse load. Wang et al. (2017) explored the soil arching procedures for planar trapdoors in cohesive-frictional soils under both active and passive situations. Recently, Shiau et al. (2021a, 2021b, 2022) studied the pipeline burst-related ground stability under collapse and blowout conditions in undrained soils. Noting that the consideration was given to no surcharge loading, the sophisticated load ratio normalization has restricted its practical uses.

* Corresponding author.
E-mail address: ksurapar@engr.tu.ac.th (S. Keawsawasvong).

https://doi.org/10.1016/j.jpse.2023.100128
Received 16 March 2023; Received in revised form 10 May 2023; Accepted 12 May 2023

The three stability factors and the principle of the superposition approach are well known and they have been often used in the determination of the bearing capacity of shallow foundations (Terzaghi, 1943). They have lately been adapted to a range of tunnel stability in drained conditions (Shiau and Al-Asadi, 2020a; 2020b; 2021). The analytical procedure is comparable to Terzaghi's bearing capacity problem, wherein the strip footing's footing capacity is made up of three terms including cohesiveness, surcharge, and soil unit weight. The stability equation is shown in Eq. (1).

$$\sigma_t = -cF_c + \sigma_s F_s + \gamma D F_\gamma \quad (1)$$

As shown in Eq. (1), the three stability factors, namely the cohesion factor F_c, the surcharge factor F_s, and the unit weight factor F_γ, were initially applied to evaluate the minimum tunnel support pressure (σ_t) in underground tunnel studies (Shiau and Al-Asadi, 2020a; Shiau et al., 2023), where c represents the cohesion, σ_s represents the surcharge, γ represents the soil unit weight and D represents the tunnel's diameter. The negative sign in the first term indicates that the cohesion strength acts against the directions of soil surcharge and self-weight in their tunnel stability problem. It is to be noted that a direct change of Eq. (1) would result in a new equation that can be used to evaluate the passive failure (i.e., blowout scenario) by using a positive cF_c, as shown in Eq. (2).

$$\sigma_t = cF_c + \sigma_s F_s + \gamma D F_\gamma \quad (2)$$

In this paper, we employed Eq. (2) to study the drained stability of passive planar trapdoor in cohesive-frictional soil by using the three stability factors approach F_c, F_s, and F_γ. The study aims to expand the stability solution for a reliable and accurate assessment of soil stability in a blowout event. This passive trapdoor problem represents the blowout stability of soils due to defective pipelines under high water main pressures. The new upper and lower bound solutions are computed through finite element limit analysis, which is one of the advanced methods nowadays for solving complex geotechnical stability problems. Numerical solutions of the three stability factors are then presented using design charts and tables for practical uses.

2. Problem statement and numerical modeling

Fig. 1 shows the problem definition of a planar passive trapdoor in cohesive-frictional soil subjected to an uplift trapdoor pressure. For the planar trapdoor, a plain strain condition is assumed, in that the length of the trapdoor (perpendicular to the plane) is infinite. The geometry is considered as a trapdoor width of B, and a depth of H from the ground surface, which is subjected to a vertical surcharge loading σ_s. The uplift uniform pressure σ_t is applied onto the trapdoor surface, i.e., acting against the surcharge loading. The soil mass is assumed to obey the Mohr-Coulomb (MC) yield criteria with the following three soil parameters, including a drained cohesion c, drained friction angle ϕ, and soil unit weight γ.

To determine the internal trapdoor pressure σ_t of the passive trapdoor problem in cohesive-frictional soil at the blowout scenario, it is proposed that Eq. (2) be used. Noting that Eq. (2) is a function of two dimensionless design parameters namely the drained friction angle ϕ and the soil cover depth ratio H/B, the three stability factors F_c, F_s, and F_γ are functions of ϕ and H/B as shown in Eq. (3).

$$F_c, F_s, F_\gamma = f\left(\phi, \frac{H}{B}\right) \quad (3)$$

One of the popular methods nowadays for solving geotechnical stability problems is Finite Element Limit Analysis (FELA) with Upper Bound (UB) and Lower Bound (LB) techniques. Sloan (2013) developed FELA to determine the soil stability of several geotechnical structures. He also reported on the early efforts of FELA that used linear programming (Sloan, 1988; 1989). The latest significant developments were based on Lyamin and Sloan (2002a, 2002b) and Krabbenhoft et al. (2007) with a nonlinear programming approach. In LB analysis, a linear three-node triangular element with nodal stresses including σ_x, σ_y, and τ_{xy} is employed as the basic unknown variables for the plane strain problem. The element must fulfill statically admissible stress discontinuities to ensure the continuity of normal and shear stresses between all elements. Furthermore, stress equilibrium and the MC yield criterion are also considered in LB analysis. The objective function is set as the passive pressure at trapdoors, and the yield criterion and stress equilibrium equations must be satisfied. Regarding UB FELA, the basic element used is a six-node triangular element in which each node possesses two fundamental unknown velocities - horizontal (u) and vertical velocities (v). Kinematically admissible velocity discontinuities are allowed at all element interfaces. To incorporate the MC model into the two fundamental unknown velocities, the associated flow rule is assumed. It is worth noting that these two fundamental unknown velocities represent tangential and normal velocity jumps along the discontinuity. Similar to LB analysis, the passive trapdoor pressure is the objective function of UB analysis.

In the geotechnical engineering field, these FELA techniques have been successfully applied to a wide range of drained and undrained stability problems (Keawsawasvong and Shiau, 2022;

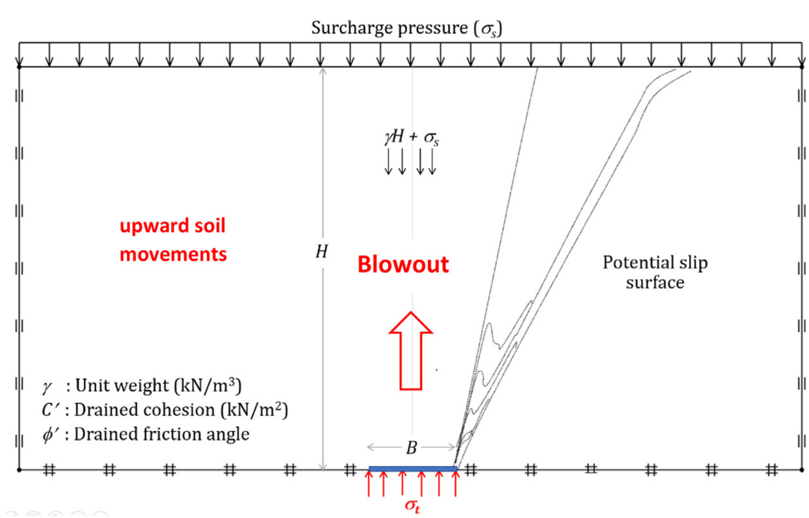

(a)

Fig. 1. Problem statement of a passive planar trapdoor in cohesive-frictional soil.

Keawsawasvong et al., 2021, 2022a,b; Keawsawasvong and Ukritchon, 2017, 2019a,b; Yodsomjai et al., 2021a,b). OptumG2 is a finite element limit analysis software that is based on the most up-to-date numerical technique (Sloan, 2013). It is employed in this study to compute the lower and upper bound limit loads of the passive trapdoor problem. In OptumG2, the upper bound elements contain three nodes providing a linear interpolation of unknown velocities whilst the lower bound element contains three nodes and a linear interpolation of unknown stresses, with stress discontinuities permitted at overlapping vertices of surrounding triangles. The solid materials following the rigid-perfectly plastic Mohr-coulomb material with an accompanying flow rule were used to simulate the drained soil. More details of the method can be found in Sloan (2013) and will not be repeated here.

In the FELA analysis, all numerical models are subjected to standard boundary conditions. As shown in Fig. 2, the bottom boundary was fixed in both x- and y-directions except for the trapdoor door which is a free surface, while the left and right boundaries were fixed in the x-direction, but free to move in the y-direction. The typical assumption for boundary conditions follows the comment setting used in the FELA or FEM of many geotechnical engineering problems. Note that both sides of the trapdoor and the bottom boundaries are rigid. Additionally, the assumption of the surface roughness of the trapdoor is fully rough because the underlying soil is set to be fully connected to the soil mass above the trapdoor. The model domain size was chosen to be big enough to ensure that the overall soil movements are well located within the chosen domain.

In all upper and lower bound analyses, both the adaptive mesh refinement and load multiplier approach were employed to reduce the bounding differences between the upper and lower bound solutions (Sloan, 2013). This adaptive mesh refinement technique is a sophisticated feature of OptumCE that adopts an automated adaptive mesh refinement approach (Ciria et al., 2008). The mesh is automatically expanded in sensitive zones with significant plastic shearing strain using adaptive mesh techniques. All numerical simulations start with an initial number of 5,000 to 10,000 elements and aim to achieve a goal of 10,000 elements after five adaptive iterations. In this study, 5,000 to 10,000 elements were used, as the accuracy of the results depends on the number of mesh elements. Employing more elements may indicate a more sensitive stress zone, leading to a more precise solution, but it is not necessary to use more than 10,000 elements as it may consume additional CPU time and computer memory with little effect on the solution. Note that, by using this setting of the adaptive mesh refinement, the LB and UB solutions are extremely close meaning that the true solutions can be obtained.

In this study, we aim to produce upper and lower bound stability factors (F_c, F_s, and F_γ) that can be used to determine critical blowout pressures and their associated passive failure modes in drained soils. These three stability factors are studied for a broad range of parameters as follows: (1) the cover depth ratios H/B = 0.5–10; and (2) the soil drained friction angle ϕ = 0–40°, and their results are discussed below.

3. Discussing the results

Numerical results of the three stability factors (F_c, F_s, and F_γ) are reported throughout the paper according to the principles of superposition using Eq. (2). To determine F_c, both $\gamma = 0$ and $\sigma_s = 0$ are assigned in all computations. F_c can then be calculated using the equation $\sigma_t = cF_c$. To compute F_s, both $\gamma = 0$ and $c = 0$ are used in the analysis. F_s is then calculated using the equation $\sigma_t = \sigma_s F_s$. To determine F_γ, both $c = 0$ and $\sigma_s = 0$ are the required input in the analysis. F_γ is then calculated using the equation $\sigma_t = \gamma B F_\gamma$. With the produced three stability factors, Eq. (2) can be used to calculate the blowout pressure for the passive trapdoor. This is not unfamiliar from Terzaghi's three bearing capacity factors and the approach of superposition.

Figs. 3–5 and Tables 1–6 show the complete upper and lower bound blowout solutions of the passive planar trapdoor in cohesive-frictional soil. In the figures, the dashed and solid lines represent the UB and LB FELA solutions, respectively. Consequently, the effect of H/D and ϕ on the three stability factors is investigated in detail. It is to be noted that the current solutions of UB and LB can bracket the "true" solution to within 1%, which has greatly enhanced the confidence in this study. It may also be prudent to conclude that all other solutions in the future produced using different methods must compare their solutions with the solutions in this paper.

For the cohesion factor F_c in Fig. 3, the concave relationship between φ and F_c is shown for the deep trapdoor ($H/B > 2$). Note that the gradient of the curve is largely affected by the depth of the trapdoor. The greater the H/B, the larger the F_c. This is mostly due to the development of soil arching in the deeper trapdoor. Nevertheless, for the shallow trapdoor ($H/B < 2$), ϕ has little to none effect on F_c. Fig. 4 shows the relationship between ϕ and F_s for the various values of H/B. The F_s values increase

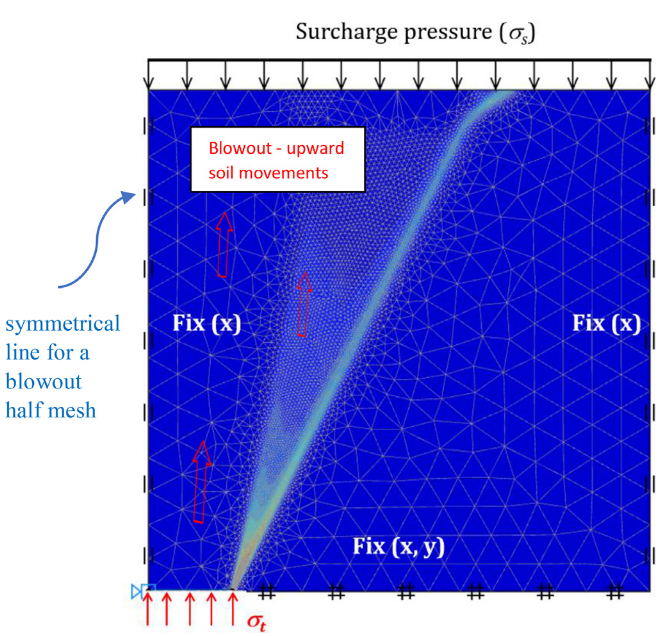

Fig. 2. A typical model with boundary condition, adaptive mesh and potential failure mechanism (symmetrical half mesh).

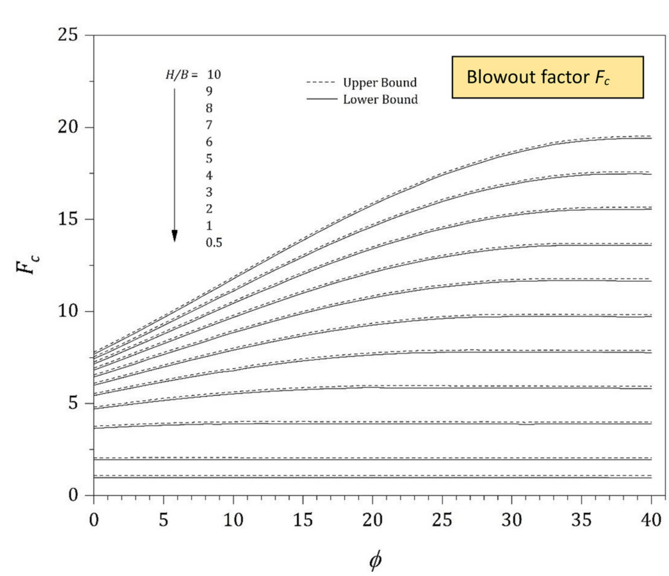

Fig. 3. F_c vs ϕ (LB and UB) for various depth ratios (H/B = 0.5–10).

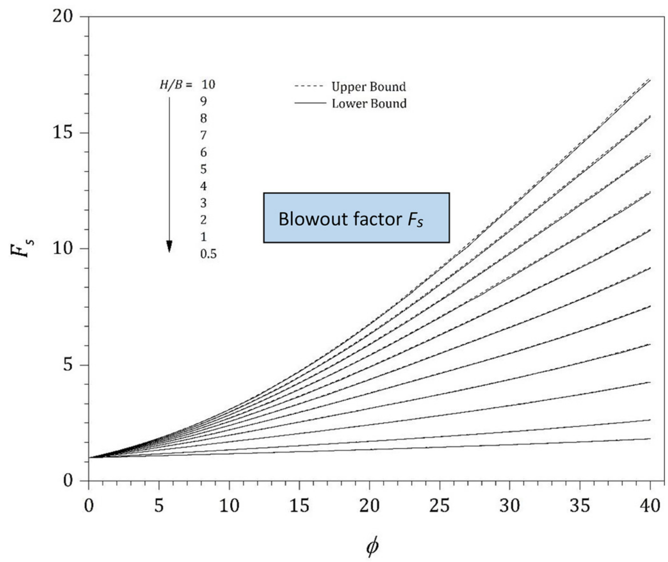

Fig. 4. F_s vs ϕ (LB and UB) for various depth ratios (H/B = 0.5–10).

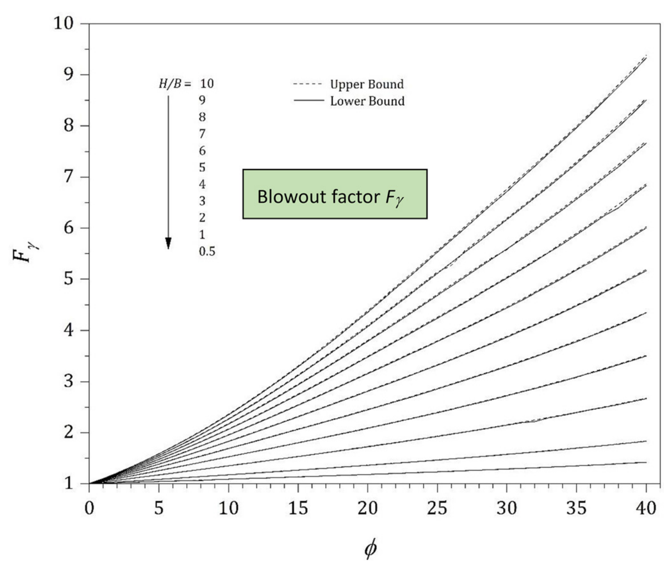

Fig. 5. F_γ vs ϕ (LB and UB) for various depth ratios (H/B = 0.5–10).

nonlinearly with ϕ. Again, a greater depth ratio H/D leads to a greater value of F_s, owning to a stronger soil arch developed in a deeper trapdoor. For the frictionless soil ($\phi = 0°$), the surcharge factor F_s is zero for all values of H/D. Finally, the effect of φ on the soil unit weight factor F_γ is shown in Fig. 5. For all the analyzed cases, Fig. 5 shows an "approximately" linearly increasing correlation between F_γ and ϕ. A minimum

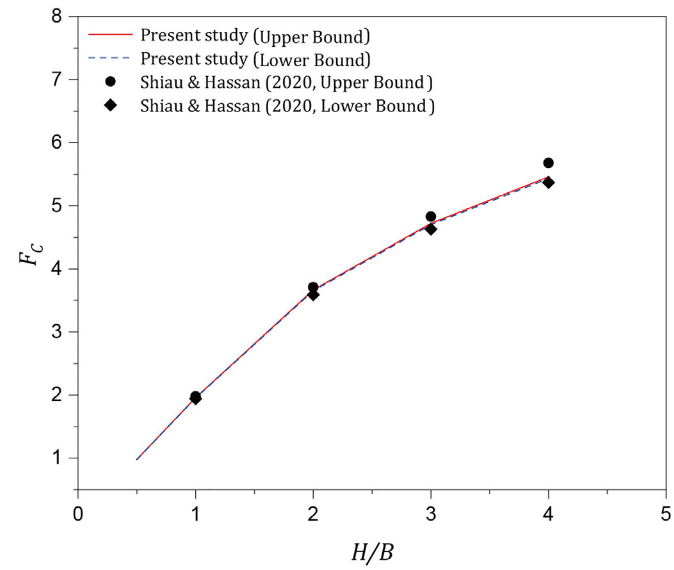

Fig. 6. Comparison of F_c between the present study and previous study (ϕ = 0°).

F_γ value of 1 is obtained for all depths of frictionless soil ($\phi = 0°$). A greater depth ratio H/D leads to a greater value of F_γ.

4. Example

For a blowout stability evaluation, an underground cavity is subject to a surcharge pressure of 100 kPa (σ_s =100 kPa). The cavity has a width (B) of 2 m and a cover depth (H) of 2 m. The soil is found to have a cohesion (c = 17 kPa) and internal friction angle φ of 10° with the soil unit weight of 16 kN/m^3. Determine the blowout pressure using the three stability factors provided in Tables 1–6.

Solution: For $H/B = 1$ and $\phi = 10°$, Tables 1, 3 and 5 provide values of lower bounds $F_c = 1.953$, $F_s = 1.344$ and $F_\gamma = 1.178$. Substituting all the parameters into Eq. (2), σ_t is calculated as 205.29 kPa ~ i.e., the value of critical blowout pressure. The actual computer analysis using the parameters gives a value of 205.23 kPa, which is very close to the table solution. This example has reinforced the confidence in using the rigorous factors provided in Tables 1–6.

5. Comparison with published results

Even though there are only a few published results available for comparison with our stability coefficients, a comparison between the present study and previous solutions can improve the confidence in using the produced results. In Fig. 6, the results of F_c are compared with the re-

Table 1
F_c vs ϕ (LB) for various depth ratios (H/B = 0.5–10).

ϕ	H/B (F_c, LB)										
	0.5	1	2	3	4	5	6	7	8	9	10
0	0.977	1.939	3.652	4.701	5.435	5.996	6.444	6.822	7.149	7.435	7.686
1	0.977	1.943	3.695	4.800	5.588	6.193	6.681	7.094	7.466	7.768	8.062
2	0.977	1.949	3.730	4.895	5.736	6.394	6.922	7.385	7.790	8.127	8.452
3	0.977	1.954	3.765	4.989	5.884	6.594	7.162	7.676	8.113	8.486	8.842
4	0.977	1.953	3.793	5.079	6.032	6.790	7.425	7.962	8.438	8.866	9.252
5	0.976	1.953	3.819	5.164	6.173	6.980	7.664	8.249	8.773	9.240	9.661
6	0.977	1.954	3.841	5.243	6.308	7.174	7.905	8.539	9.102	9.613	10.076

(continued on next page)

Table 1 (*continued*)

ϕ	H/B (F_c, LB)										
	0.5	1	2	3	4	5	6	7	8	9	10
7	0.977	1.953	3.863	5.319	6.445	7.362	8.133	8.827	9.424	9.986	10.490
8	0.977	1.953	3.887	5.391	6.572	7.544	8.367	9.117	9.776	10.364	10.919
9	0.977	1.953	3.875	5.462	6.696	7.728	8.624	9.398	10.108	10.752	11.336
10	0.976	1.953	3.898	5.524	6.778	7.900	8.854	9.680	10.441	11.098	11.770
11	0.976	1.952	3.908	5.579	6.927	8.068	9.063	9.953	10.768	11.498	12.199
12	0.976	1.952	3.910	5.633	7.034	8.225	9.278	10.223	11.086	11.878	12.612
13	0.976	1.952	3.906	5.677	7.133	8.383	9.491	10.486	11.384	12.251	13.041
14	0.976	1.952	3.904	5.717	7.227	8.529	9.698	10.747	11.715	12.604	13.452
15	0.976	1.952	3.905	5.753	7.315	8.674	9.895	10.999	12.020	12.960	13.860
16	0.976	1.952	3.904	5.786	7.393	8.807	10.078	11.237	12.320	13.326	14.266
17	0.976	1.952	3.903	5.806	7.467	8.934	10.264	11.478	12.611	13.665	14.657
18	0.976	1.952	3.903	5.823	7.535	9.044	10.425	11.698	12.879	13.991	15.053
19	0.976	1.952	3.903	5.860	7.591	9.158	10.583	11.907	13.156	14.320	15.424
20	0.976	1.951	3.903	5.868	7.640	9.257	10.738	12.116	13.405	14.616	15.779
21	0.976	1.951	3.899	5.850	7.686	9.348	10.882	12.309	13.646	14.918	16.133
22	0.976	1.950	3.902	5.852	7.721	9.423	11.001	12.486	13.864	15.201	16.465
23	0.975	1.950	3.900	5.852	7.755	9.500	11.123	12.651	14.083	15.466	16.765
24	0.975	1.950	3.899	5.852	7.769	9.558	11.234	12.810	14.301	15.719	17.102
25	0.974	1.950	3.898	5.850	7.774	9.614	11.323	12.940	14.487	15.974	17.401
26	0.974	1.949	3.899	5.849	7.788	9.653	11.407	13.069	14.651	16.190	17.654
27	0.974	1.949	3.897	5.847	7.798	9.687	11.472	13.185	14.827	16.396	17.907
28	0.974	1.949	3.898	5.848	7.795	9.713	11.542	13.285	14.967	16.584	18.138
29	0.974	1.948	3.896	5.844	7.793	9.715	11.593	13.379	15.102	16.754	18.382
30	0.974	1.948	3.895	5.846	7.790	9.730	11.629	13.444	15.207	16.892	18.563
31	0.974	1.948	3.864	5.846	7.779	9.739	11.647	13.506	15.311	17.048	18.744
32	0.974	1.947	3.893	5.843	7.790	9.738	11.667	13.551	15.378	17.156	18.907
33	0.973	1.947	3.891	5.841	7.790	9.735	11.673	13.577	15.449	17.261	19.074
34	0.973	1.947	3.890	5.840	7.783	9.734	11.675	13.593	15.491	17.341	19.174
35	0.973	1.947	3.889	5.839	7.782	9.730	11.675	13.595	15.523	17.405	19.255
36	0.973	1.945	3.888	5.838	7.781	9.728	11.679	13.591	15.538	17.451	19.315
37	0.972	1.945	3.885	5.836	7.777	9.722	11.662	13.591	15.548	17.467	19.366
38	0.972	1.944	3.884	5.825	7.774	9.710	11.661	13.589	15.548	17.468	19.391
39	0.972	1.943	3.884	5.824	7.772	9.716	11.660	13.588	15.550	17.480	19.409
40	0.972	1.943	3.882	5.823	7.770	9.717	11.659	13.587	15.553	17.455	19.414

Table 2
F_c vs ϕ (UB) for various depth ratios (H/B = 0.5–10).

ϕ	H/B (F_c, UB)										
	0.5	1	2	3	4	5	6	7	8	9	10
0	0.979	1.959	3.667	4.721	5.459	6.023	6.479	6.859	7.187	7.472	7.726
1	0.979	1.959	3.707	4.821	5.613	6.225	6.723	7.143	7.505	7.824	8.108
2	0.979	1.959	3.743	4.917	5.764	6.426	6.969	7.431	7.831	8.186	8.504
3	0.979	1.959	3.778	5.012	5.914	6.626	7.214	7.718	8.157	8.547	8.900
4	0.979	1.959	3.808	5.101	6.059	6.823	7.460	8.008	8.489	8.918	9.307
5	0.979	1.959	3.835	5.187	6.202	7.019	7.706	8.299	8.824	9.294	9.722
6	0.979	1.959	3.858	5.268	6.340	7.211	7.950	8.591	9.160	9.674	10.141
7	0.979	1.959	3.877	5.345	6.475	7.401	8.189	8.881	9.497	10.056	10.565
8	0.979	1.959	3.892	5.417	6.604	7.586	8.428	9.169	9.835	10.438	10.993
9	0.979	1.958	3.904	5.484	6.729	7.766	8.662	9.460	10.171	10.822	11.423
10	0.979	1.958	3.912	5.547	6.847	7.941	8.893	9.738	10.503	11.204	11.851
11	0.979	1.958	3.915	5.604	6.960	8.111	9.116	10.016	10.835	11.584	12.281
12	0.979	1.958	3.916	5.655	7.068	8.275	9.336	10.289	11.160	11.963	12.709
13	0.979	1.958	3.916	5.708	7.169	8.431	9.547	10.557	11.480	12.336	13.135
14	0.979	1.958	3.916	5.742	7.264	8.580	9.753	10.816	11.796	12.703	13.554
15	0.979	1.958	3.915	5.777	7.351	8.722	9.949	11.069	12.103	13.063	13.968
16	0.979	1.957	3.915	5.807	7.431	8.856	10.139	11.314	12.400	13.416	14.375
17	0.979	1.957	3.915	5.832	7.504	8.983	10.319	11.547	12.689	13.762	14.773
18	0.979	1.957	3.915	5.849	7.569	9.100	10.489	11.772	12.969	14.097	15.162
19	0.979	1.957	3.914	5.862	7.629	9.208	10.652	11.987	13.238	14.419	15.541
20	0.978	1.957	3.914	5.869	7.679	9.307	10.803	12.190	13.493	14.726	15.907
21	0.978	1.957	3.914	5.870	7.723	9.398	10.942	12.382	13.741	15.027	16.256
22	0.978	1.957	3.913	5.870	7.758	9.476	11.070	12.563	13.970	15.311	16.597
23	0.978	1.956	3.913	5.869	7.786	9.549	11.190	12.730	14.189	15.581	16.919

(*continued on next page*)

Table 2 (*continued*)

ϕ	H/B (F_c, UB)										
	0.5	1	2	3	4	5	6	7	8	9	10
24	0.978	1.956	3.912	5.869	7.806	9.611	11.297	12.884	14.395	15.838	17.224
25	0.978	1.956	3.912	5.868	7.818	9.663	11.392	13.024	14.584	16.076	17.517
26	0.978	1.956	3.911	5.867	7.823	9.705	11.475	13.154	14.758	16.301	17.791
27	0.978	1.955	3.911	5.866	7.822	9.737	11.546	13.268	14.919	16.507	18.043
28	0.978	1.955	3.911	5.866	7.821	9.759	11.606	13.368	15.062	16.695	18.275
29	0.977	1.955	3.910	5.865	7.821	9.774	11.653	13.454	15.190	16.865	18.493
30	0.977	1.955	3.910	5.865	7.819	9.773	11.691	13.527	15.301	17.018	18.691
31	0.977	1.954	3.909	5.864	7.818	9.772	11.714	13.585	15.395	17.154	18.864
32	0.977	1.954	3.909	5.863	7.817	9.772	11.724	13.629	15.475	17.269	19.020
33	0.977	1.954	3.909	5.862	7.817	9.771	11.724	13.657	15.537	17.366	19.154
34	0.977	1.954	3.908	5.861	7.814	9.768	11.726	13.673	15.584	17.445	19.271
35	0.977	1.954	3.907	5.860	7.814	9.767	11.722	13.675	15.613	17.506	19.364
36	0.977	1.953	3.907	5.860	7.813	9.767	11.719	13.671	15.626	17.550	19.434
37	0.976	1.953	3.906	5.859	7.812	9.764	11.720	13.671	15.626	17.571	19.487
38	0.976	1.953	3.906	5.858	7.811	9.765	11.718	13.669	15.623	17.575	19.518
39	0.976	1.953	3.905	5.857	7.810	9.764	11.715	13.668	15.622	17.576	19.521
40	0.976	1.952	3.905	5.856	7.809	9.763	11.712	13.667	15.623	17.577	19.524

Table 3
F_s vs ϕ (LB) for various depth ratios (H/B = 0.5–10).

ϕ	H/B (F_s, LB)										
	0.5	1	2	3	4	5	6	7	8	9	10
0	1.000	1.000	1.000	1.000	1.000	1.000	1.000	1.000	1.000	1.000	0.999
1	1.017	1.034	1.064	1.084	1.098	1.108	1.117	1.124	1.130	1.136	1.141
2	1.034	1.068	1.130	1.171	1.200	1.223	1.242	1.258	1.272	1.284	1.295
3	1.051	1.102	1.197	1.261	1.308	1.346	1.376	1.402	1.425	1.445	1.464
4	1.068	1.137	1.265	1.355	1.422	1.475	1.519	1.557	1.590	1.618	1.647
5	1.085	1.170	1.334	1.452	1.538	1.611	1.670	1.722	1.768	1.808	1.845
6	1.103	1.205	1.404	1.551	1.663	1.754	1.831	1.897	1.957	2.010	2.059
7	1.120	1.240	1.474	1.653	1.791	1.904	2.000	2.084	2.159	2.227	2.287
8	1.137	1.274	1.545	1.751	1.924	2.060	2.180	2.278	2.373	2.458	2.535
9	1.155	1.309	1.616	1.865	2.054	2.224	2.363	2.489	2.601	2.703	2.798
10	1.172	1.344	1.687	1.974	2.201	2.393	2.559	2.707	2.839	2.962	3.076
11	1.190	1.379	1.759	2.084	2.347	2.568	2.762	2.925	3.093	3.235	3.368
12	1.208	1.415	1.830	2.197	2.494	2.750	2.972	3.173	3.356	3.525	3.667
13	1.225	1.451	1.901	2.310	2.648	2.935	3.191	3.407	3.633	3.828	4.012
14	1.243	1.486	1.974	2.426	2.803	3.127	3.416	3.679	3.922	4.132	4.356
15	1.260	1.523	2.046	2.542	2.960	3.324	3.640	3.947	4.222	4.476	4.714
16	1.278	1.560	2.119	2.657	3.119	3.526	3.890	4.222	4.531	4.819	5.093
17	1.298	1.597	2.194	2.775	3.283	3.718	4.136	4.508	4.850	5.176	5.476
18	1.317	1.634	2.268	2.893	3.447	3.940	4.376	4.802	5.182	5.547	5.886
19	1.336	1.672	2.344	3.002	3.614	4.154	4.646	5.104	5.528	5.926	6.312
20	1.355	1.710	2.421	3.129	3.782	4.369	4.907	5.409	5.875	6.322	6.747
21	1.374	1.749	2.498	3.246	3.950	4.589	5.174	5.723	6.235	6.725	7.194
22	1.394	1.788	2.576	3.363	4.120	4.805	5.438	6.046	6.606	7.142	7.655
23	1.413	1.828	2.656	3.483	4.291	5.032	5.721	6.370	6.980	7.572	8.114
24	1.434	1.868	2.737	3.604	4.460	5.257	5.996	6.704	7.366	7.997	8.614
25	1.454	1.909	2.818	3.728	4.629	5.482	6.284	7.035	7.757	8.443	9.100
26	1.475	1.951	2.902	3.850	4.799	5.710	6.565	7.377	8.150	8.896	9.613
27	1.497	1.993	2.986	3.979	4.973	5.935	6.848	7.721	8.554	9.344	10.083
28	1.518	2.036	3.071	4.108	5.144	6.164	7.139	8.037	8.957	9.820	10.651
29	1.538	2.080	3.161	4.241	5.322	6.393	7.424	8.399	9.372	10.287	11.188
30	1.562	2.125	3.248	4.374	5.496	6.617	7.714	8.746	9.775	10.760	11.714
31	1.583	2.170	3.336	4.511	5.676	6.850	8.001	9.111	10.195	11.239	12.259
32	1.608	2.215	3.434	4.660	5.867	7.083	8.291	9.462	10.611	11.724	12.805
33	1.632	2.264	3.529	4.787	6.054	7.322	8.581	9.817	11.028	12.205	13.362
34	1.656	2.314	3.626	4.939	6.246	7.564	8.871	10.178	11.435	12.700	13.905
35	1.681	2.363	3.726	5.088	6.451	7.814	9.167	10.522	11.877	13.190	14.465
36	1.707	2.414	3.827	5.240	6.651	8.065	9.468	10.891	12.286	13.665	15.009
37	1.733	2.466	3.932	5.400	6.859	8.324	9.792	11.262	12.720	14.156	15.578
38	1.759	2.520	4.038	5.540	7.076	8.584	10.117	11.614	13.150	14.670	16.147
39	1.787	2.574	4.149	5.724	7.296	8.864	10.438	12.004	13.589	15.153	16.725
40	1.816	2.631	4.262	5.890	7.522	9.158	10.784	12.410	14.013	15.680	17.269

Table 4
F_s vs ϕ (UB) for various depth ratios (H/B = 0.5–10).

ϕ	H/B (F_s, UB)										
	0.5	1	2	3	4	5	6	7	8	9	10
0	1.000	1.000	1.000	1.000	1.000	1.000	1.000	1.000	1.000	1.000	1.000
1	1.017	1.034	1.065	1.084	1.098	1.109	1.117	1.125	1.131	1.137	1.142
2	1.034	1.068	1.131	1.172	1.201	1.224	1.243	1.259	1.273	1.286	1.297
3	1.051	1.103	1.198	1.263	1.310	1.347	1.378	1.404	1.427	1.448	1.466
4	1.068	1.137	1.266	1.358	1.424	1.477	1.522	1.560	1.593	1.624	1.651
5	1.086	1.171	1.335	1.454	1.543	1.614	1.674	1.726	1.772	1.813	1.850
6	1.103	1.206	1.405	1.554	1.666	1.758	1.835	1.903	1.963	2.017	2.066
7	1.120	1.240	1.476	1.656	1.795	1.909	2.005	2.090	2.166	2.234	2.297
8	1.138	1.275	1.547	1.761	1.928	2.066	2.184	2.289	2.382	2.467	2.545
9	1.155	1.310	1.618	1.869	2.066	2.230	2.372	2.497	2.611	2.714	2.809
10	1.173	1.345	1.690	1.978	2.207	2.400	2.568	2.717	2.852	2.975	3.090
11	1.190	1.381	1.761	2.089	2.353	2.577	2.772	2.947	3.106	3.252	3.387
12	1.208	1.416	1.832	2.202	2.502	2.758	2.984	3.187	3.372	3.542	3.701
13	1.226	1.452	1.904	2.316	2.655	2.946	3.204	3.437	3.650	3.848	4.032
14	1.244	1.488	1.976	2.431	2.811	3.139	3.431	3.696	3.941	4.167	4.379
15	1.262	1.524	2.049	2.548	2.969	3.337	3.665	3.966	4.242	4.500	4.743
16	1.281	1.561	2.123	2.665	3.130	3.539	3.907	4.244	4.555	4.847	5.121
17	1.299	1.598	2.197	2.783	3.294	3.746	4.155	4.530	4.879	5.207	5.516
18	1.318	1.636	2.272	2.900	3.459	3.956	4.408	4.825	5.214	5.580	5.926
19	1.337	1.674	2.348	3.018	3.627	4.170	4.667	5.127	5.558	5.964	6.350
20	1.356	1.712	2.424	3.136	3.795	4.387	4.931	5.437	5.911	6.360	6.788
21	1.375	1.751	2.502	3.253	3.964	4.607	5.200	5.753	6.274	6.768	7.240
22	1.395	1.790	2.581	3.371	4.134	4.829	5.473	6.075	6.644	7.186	7.705
23	1.415	1.830	2.661	3.491	4.305	5.053	5.750	6.404	7.023	7.615	8.181
24	1.435	1.871	2.742	3.613	4.475	5.278	6.029	6.736	7.408	8.051	8.669
25	1.456	1.912	2.824	3.736	4.645	5.506	6.311	7.074	7.800	8.496	9.168
26	1.477	1.954	2.908	3.861	4.815	5.734	6.596	7.415	8.198	8.950	9.676
27	1.498	1.996	2.992	3.988	4.984	5.962	6.883	7.760	8.600	9.409	10.194
28	1.520	2.039	3.079	4.119	5.158	6.188	7.171	8.108	9.010	9.876	10.717
29	1.542	2.084	3.167	4.250	5.334	6.416	7.459	8.458	9.419	10.349	11.250
30	1.564	2.128	3.257	4.385	5.514	6.643	7.748	8.809	9.835	10.826	11.789
31	1.587	2.174	3.349	4.523	5.697	6.871	8.037	9.163	10.250	11.306	12.334
32	1.610	2.221	3.442	4.663	5.884	7.105	8.326	9.516	10.668	11.790	12.884
33	1.634	2.269	3.538	4.806	6.074	7.344	8.614	9.869	11.090	12.278	13.439
34	1.659	2.318	3.635	4.953	6.271	7.589	8.905	10.222	11.512	12.766	13.996
35	1.684	2.368	3.735	5.103	6.471	7.839	9.207	10.575	11.934	13.256	14.558
36	1.706	2.419	3.838	5.257	6.677	8.096	9.514	10.934	12.352	13.751	15.061
37	1.736	2.471	3.944	5.415	6.887	8.358	9.829	11.300	12.773	14.241	15.682
38	1.763	2.526	4.051	5.578	7.103	8.629	10.154	11.679	13.203	14.730	16.248
39	1.790	2.581	4.162	5.743	7.324	8.905	10.487	12.067	13.650	15.231	16.810
40	1.819	2.638	4.276	5.914	7.552	9.190	10.830	12.467	14.104	15.741	17.382

Table 5
F_γ vs ϕ (LB) for various depth ratios (H/B = 0.5–10).

ϕ	H/B (F_γ, LB)										
	0.5	1	2	3	4	5	6	7	8	9	10
0	1.000	1.000	1.000	1.000	1.000	1.000	1.000	1.000	1.000	1.000	1.008
1	1.009	1.017	1.035	1.050	1.062	1.072	1.080	1.086	1.092	1.098	1.103
2	1.017	1.035	1.070	1.101	1.126	1.146	1.163	1.178	1.190	1.202	1.212
3	1.026	1.052	1.105	1.153	1.191	1.223	1.250	1.274	1.294	1.313	1.329
4	1.035	1.070	1.139	1.205	1.259	1.303	1.341	1.374	1.404	1.430	1.454
5	1.044	1.087	1.174	1.258	1.327	1.385	1.435	1.479	1.519	1.553	1.585
6	1.052	1.105	1.210	1.311	1.397	1.470	1.533	1.589	1.638	1.684	1.726
7	1.061	1.122	1.245	1.365	1.469	1.557	1.634	1.702	1.764	1.820	1.872
8	1.064	1.140	1.280	1.419	1.541	1.646	1.738	1.820	1.895	1.962	2.025
9	1.079	1.158	1.315	1.473	1.614	1.737	1.846	1.942	2.030	2.112	2.185
10	1.088	1.176	1.351	1.526	1.689	1.830	1.954	2.068	2.170	2.266	2.353
11	1.097	1.194	1.387	1.582	1.763	1.923	2.067	2.197	2.316	2.426	2.527
12	1.106	1.212	1.424	1.636	1.839	2.019	2.182	2.328	2.464	2.590	2.710
13	1.115	1.230	1.460	1.690	1.914	2.116	2.299	2.464	2.617	2.762	2.899
14	1.124	1.248	1.496	1.745	1.990	2.214	2.417	2.604	2.776	2.939	3.092
15	1.133	1.267	1.533	1.801	2.067	2.312	2.537	2.745	2.938	3.118	3.292
16	1.143	1.285	1.570	1.857	2.140	2.412	2.658	2.887	3.103	3.307	3.498
17	1.152	1.304	1.609	1.913	2.217	2.510	2.782	3.033	3.272	3.494	3.700
18	1.162	1.323	1.647	1.971	2.292	2.611	2.908	3.182	3.440	3.688	3.915
19	1.171	1.343	1.686	2.027	2.371	2.710	3.032	3.333	3.612	3.879	4.139
20	1.181	1.362	1.724	2.088	2.450	2.812	3.156	3.482	3.791	4.079	4.359
21	1.191	1.382	1.764	2.147	2.529	2.911	3.280	3.631	3.965	4.284	4.590
22	1.201	1.402	1.803	2.208	2.609	3.010	3.404	3.787	4.143	4.489	4.821

(continued on next page)

Table 5 (*continued*)

ϕ	H/B (F_γ, LB)										
	0.5	1	2	3	4	5	6	7	8	9	10
23	1.211	1.423	1.845	2.267	2.687	3.113	3.533	3.935	4.322	4.696	5.049
24	1.221	1.443	1.886	2.330	2.770	3.218	3.656	4.088	4.505	4.904	5.286
25	1.232	1.464	1.928	2.390	2.856	3.321	3.786	4.239	4.686	5.114	5.528
26	1.243	1.486	1.970	2.455	2.942	3.426	3.916	4.394	4.861	5.322	5.765
27	1.254	1.507	2.013	2.522	3.030	3.536	4.041	4.548	5.045	5.532	6.002
28	1.264	1.529	2.058	2.586	3.118	3.645	4.174	4.704	5.229	5.738	6.246
29	1.276	1.551	2.103	2.654	3.205	3.755	4.310	4.863	5.410	5.954	6.485
30	1.287	1.575	2.149	2.725	3.298	3.871	4.443	5.021	5.591	6.170	6.716
31	1.299	1.598	2.195	2.795	3.390	3.989	4.581	5.184	5.776	6.378	6.966
32	1.311	1.622	2.217	2.865	3.485	4.106	4.729	5.349	5.966	6.595	7.210
33	1.323	1.645	2.291	2.938	3.585	4.230	4.872	5.523	6.162	6.808	7.463
34	1.336	1.671	2.340	3.010	3.683	4.353	5.020	5.688	6.362	7.036	7.711
35	1.348	1.697	2.392	3.090	3.782	4.483	5.181	5.871	6.568	7.262	7.965
36	1.361	1.722	2.450	3.168	3.890	4.610	5.330	6.055	6.772	7.504	8.225
37	1.374	1.749	2.498	3.244	3.996	4.745	5.494	6.243	6.992	7.734	8.497
38	1.389	1.776	2.552	3.330	4.107	4.883	5.661	6.395	7.196	7.981	8.764
39	1.404	1.804	2.610	3.414	4.218	5.024	5.825	6.627	7.435	8.238	9.040
40	1.417	1.833	2.666	3.501	4.348	5.164	6.005	6.831	7.661	8.504	9.330

Table 6
F_γ vs ϕ (UB) for various depth ratios (H/B = 0.5–10).

ϕ	H/B (F_γ, UB)										
	0.5	1	2	3	4	5	6	7	8	9	10
0	1.000	1.000	1.000	1.000	1.008	1.000	1.000	1.000	1.000	1.000	1.000
1	1.009	1.017	1.035	1.050	1.062	1.072	1.080	1.087	1.093	1.098	1.103
2	1.017	1.035	1.070	1.102	1.126	1.147	1.164	1.179	1.192	1.203	1.214
3	1.026	1.052	1.105	1.154	1.192	1.224	1.251	1.275	1.296	1.315	1.332
4	1.035	1.070	1.140	1.206	1.260	1.305	1.343	1.376	1.406	1.433	1.457
5	1.044	1.088	1.175	1.259	1.329	1.387	1.438	1.482	1.521	1.557	1.590
6	1.053	1.105	1.210	1.313	1.399	1.473	1.536	1.592	1.642	1.688	1.730
7	1.061	1.123	1.246	1.367	1.471	1.560	1.638	1.706	1.769	1.825	1.877
8	1.070	1.141	1.281	1.421	1.544	1.650	1.742	1.825	1.900	1.969	2.032
9	1.079	1.158	1.317	1.475	1.618	1.741	1.850	1.948	2.037	2.119	2.194
10	1.088	1.176	1.353	1.529	1.692	1.834	1.960	2.074	2.178	2.274	2.363
11	1.097	1.194	1.389	1.583	1.767	1.929	2.073	2.204	2.324	2.436	2.539
12	1.106	1.213	1.425	1.638	1.843	2.025	2.189	2.338	2.475	2.603	2.722
13	1.115	1.231	1.462	1.693	1.919	2.122	2.306	2.474	2.630	2.775	2.911
14	1.125	1.249	1.499	1.748	1.995	2.220	2.425	2.614	2.788	2.952	3.106
15	1.134	1.268	1.536	1.804	2.071	2.319	2.546	2.756	2.951	3.134	3.307
16	1.143	1.287	1.574	1.860	2.147	2.419	2.668	2.900	3.117	3.320	3.513
17	1.153	1.306	1.611	1.917	2.223	2.519	2.792	3.047	3.285	3.511	3.725
18	1.162	1.325	1.650	1.975	2.300	2.619	2.917	3.195	3.456	3.705	3.941
19	1.172	1.344	1.689	2.033	2.377	2.719	3.042	3.345	3.631	3.902	4.162
20	1.182	1.364	1.728	2.092	2.456	2.819	3.168	3.496	3.807	4.103	4.386
21	1.192	1.384	1.768	2.151	2.535	2.919	3.294	3.647	3.985	4.306	4.615
22	1.202	1.404	1.808	2.212	2.616	3.020	3.420	3.801	4.164	4.512	4.846
23	1.212	1.424	1.849	2.273	2.697	3.122	3.546	3.954	4.344	4.719	5.080
24	1.223	1.445	1.890	2.335	2.780	3.226	3.670	4.107	4.525	4.927	5.316
25	1.233	1.466	1.932	2.399	2.865	3.330	3.797	4.261	4.707	5.138	5.555
26	1.244	1.488	1.975	2.463	2.950	3.438	3.925	4.413	4.889	5.266	5.795
27	1.255	1.504	2.015	2.528	3.037	3.546	4.056	4.565	5.071	5.560	6.036
28	1.266	1.531	2.063	2.595	3.126	3.657	4.189	4.720	5.252	5.772	6.279
29	1.277	1.553	2.108	2.662	3.216	3.770	4.324	4.878	5.432	5.983	6.520
30	1.289	1.577	2.154	2.731	3.308	3.885	4.462	5.039	5.576	6.192	6.762
31	1.300	1.600	2.201	2.801	3.402	4.002	4.603	5.203	5.803	6.404	7.004
32	1.312	1.624	2.249	2.873	3.497	4.122	4.747	5.370	5.995	6.619	7.244
33	1.324	1.649	2.298	2.947	3.596	4.245	4.893	5.529	6.191	6.840	7.488
34	1.337	1.674	2.348	3.022	3.696	4.370	5.043	5.718	6.391	7.064	7.740
35	1.350	1.700	2.399	3.080	3.798	4.498	5.197	5.897	6.597	7.296	7.995
36	1.363	1.726	2.452	3.178	3.893	4.630	5.355	6.081	6.806	7.532	8.258
37	1.376	1.753	2.505	3.258	4.011	4.764	5.517	6.269	7.023	7.774	8.528
38	1.391	1.781	2.561	3.341	4.122	4.902	5.683	6.463	7.243	8.024	8.805
39	1.407	1.809	2.618	3.427	4.235	5.045	5.853	6.662	7.472	8.280	9.088
40	1.419	1.838	2.676	3.514	4.352	5.190	6.028	6.866	7.705	8.540	9.383

cently reported solutions by Shiau and Hassan (2020) for the cases of passive trapdoors in undrained soils with $\phi = 0^{\circ}$. It is found that both solutions are almost identical so that a good agreement between them can be obtained. As far as we know, no published solutions of passive trapdoor stability for F_s and F_γ exist for us to compare our current results with.

6. Conclusion

The problem of water mains blowout was investigated in this paper using the classical passive planar trapdoor, the three stability factors approach, and the principle of superposition. The upper and lower bound finite element limit analysis are the key tools for the proposed study to produce comprehensive stability factors. All numerical results, including upper and lower bound solutions of the three factors, are presented in forms of design charts and tables that can be used efficiently and effectively to estimate blowout pressures for various trapdoor depth ratios and soil friction angles. A simple example is illustrated on how to use the three stability factors. It was concluded that the obtained results offer a simple yet efficient and effective alternative way to enhance conventional designs for passive planar trapdoors in cohesive-frictional soil. The solutions presented in this study are applicable only to planar trapdoors in homogeneous soils and cannot be extended to rectangular or circular trapdoors or trapdoors in layered soils. Future study may include a 2D axisymmetric study as well as a full 3D blowout analysis using the proposed superposition approach.

Declaration of Competing Interest

The authors declare that they have no known competing financial interests or personal relationships that could have appeared to influence the work reported in this paper.

CRediT authorship contribution statement

Jim Shiau: Conceptualization, Writing – original draft, Writing – review & editing, Supervision, Resources. **Suraparb Keawsawasvong:** Conceptualization, Writing – review & editing, Data curation, Formal analysis. **Rungkhun Banyong:** Software, Writing – original draft, Investigation, Methodology, Formal analysis, Data curation.

Acknowledgment

This study was supported by Thammasat University Research Fund, Contract No. TUFT 19/2566. Also, this work was supported by the Thailand Science Research and Innovation Fundamental Fund fiscal year 2023.

References

Ciria, H., Peraire, J., Bonet, J., 2008. Mesh adaptive computation of upper and lower bounds in limit analysis. Int. J. Numer. Methods Eng. 75, 899–944.

Das, B.M., Shin, E.C., Dass, R.N., Omar, MT., 1994. Suction force below plate anchors in soft clay. Mar. Georesour. Geotechnol. 12, 71–81.

Das, BM., 1978. Model tests for uplift capacity of foundations in clay. Soil Found. 18 (2), 17–24.

Das, BM., 1980. A procedure for estimation of ultimate capacity of foundations in clay. Soil Found. 20 (1), 77–82.

Keawsawasvong, S., Shiau, J., 2022. Stability of active trapdoors in axisymmetry. Undergr. Sp. 7 (1), 50–57.

Keawsawasvong, S., Ukritchon, B., 2017. Undrained lateral capacity of I-shaped concrete piles. Songklanakarin J. Sci. Technol. 39 (6), 751–758.

Keawsawasvong, S., Ukritchon, B., 2019a. Undrained basal stability of braced circular excavations in non-homogeneous clays with linear increase of strength with depth. Comput. Geotech. 115, 103180.

Keawsawasvong, S., Ukritchon, B., 2019b. Undrained stability of a spherical cavity in cohesive soils using finite element limit analysis. J. Rock Mech. Geotech. Eng. 11 (6), 1274–1285.

Keawsawasvong, S., Thongchom, C., Likitlersuang, S., 2021. Bearing capacity of strip footing on Hoek-Brown rock mass subjected to eccentric and inclined loading. Transp. Infrastruct. Geotechnol. 8, 189–200.

Keawsawasvong, S., Shiau, J., Yoonirundorn, K., 2022a. Bearing capacity of cylindrical caissons in cohesive-frictional soils using axisymmetric finite element limit analysis. Geotech. Geol. Eng. 40, 3929–3941.

Keawsawasvong, S., Shiau, J., Limpanawannakul, K., Panomchaivath, S., 2022b. Stability charts for closely spaced strip footings on Hoek–Brown rock mass. Geotech. Geol. Eng. 40, 3051–3066 Geotech Geol Eng2022.

Koutsabeloulis, N.C., Griffiths, DV., 1989. Numerical modelling of the trap door problem. Geotechnique 39 (1), 77–89.

Krabbenhoft, K., Lyamin, A.V., Sloan, S.W., 2007. Formulation and solution of some plasticity problems as conic programs. Int. J. Solids Struct. 44 (5), 1533–1549.

Kupferman M. The vertical holding capacity of marine anchors in clay subjected to static and cyclic loading. MSc thesis, Amherst, Mass: University of Massachusetts; 1965.

Lyamin, A.V., Sloan, S.W., 2002a. Lower bound limit analysis using non-linear programming. Int. J. Numer. Methods Eng. 55 (5), 573–611.

Lyamin, A.V., Sloan, S.W., 2002b. Upper bound limit analysis using linear finite elements and non-linear programming. Int. J. Numer. Anal. Methods Geomech. 26 (2), 181–216.

Martin, CM., 2009. Undrained collapse of a shallow plane-strain trapdoor. Géotechnique 59 (10), 855–863.

Meyerhof, G.G., Adams, JI., 1968. The ultimate uplift capacity of foundations. Can. Geotech. J. 5 (4), 225–244.

Meyerhof, GG., 1973. Uplift resistance of inclined anchors and piles. In: Proceedings of the Eighth International Conference on Soil Mechanics and Foundation Engineering, 2, Moscow, pp. 167–172.

Shiau, J.&., Al-Asadi, F., 2020a. Two-dimensional tunnel heading stability factors F_c, F_s and F_γ. Tunn. Undergr. Sp. Technol. 97, 103293.

Shiau, J.&., Al-Asadi, F., 2020b. Determination of critical tunnel heading pressures using stability factors. Comput. Geotech. 119, 103345.

Shiau, J., Al-Asadi, F., 2021. Twin tunnels stability factors Fc, Fs and Fc. Geotechn. Geol. Eng. 39 (1), 335–345.

Shiau, J., Hassan, M.M., 2020. Undrained stability of active and passive trapdoors. Geotech. Res. 7, 40–48. doi:10.1680/jgere.19.00033.

Shiau, J., Chudal, B., Mahalingasivam, K., Keawsawasvong, S., 2021a. Pipeline burst-related ground stability in blowout condition. Transp. Geotech. 29, 100587.

Shiau, J., Keawsawasvong, S., Chudal, B., Mahalingasivam, K., Seehavong, S., 2021b. Sinkhole stability in elliptical cavity under collapse and blowout conditions. Geosciences 11 (10), 421.

Shiau, J., Chudal, B., Mahalingasivam, K., Keawsawasvong, S., 2022. Pipeline burst-related soil stability in collapse condition. J. Pipeline Syst. Eng. Pract. ASCE 13 (3), 04022019.

Shiau, J., Keawsawasvong, S., Al-Asadi, F., 2023. Use of Terzaghi's superposition approach for estimating critical supporting pressures in circular tunnels. Transp. Infrastruct. Geotechnol. doi:10.1007/s40515-023-00282-6.

Sloan, S.W., 1988. Lower bound limit analysis using finite elements and linear programming. Int. J. Numer. Anal. Methods Geomech. 12 (1), 61–77.

Sloan, S.W., 1989. Upper bound limit analysis using finite elements and linear programming. Int. J. Numer. Anal. Methods Geomech. 13 (3), 263–282.

Sloan, S.W., 2013. Geotechnical stability analysis. Geotechnique 63 (7), 531–537.

Smith, CC., 1998. Limit loads for an anchor/trapdoor embedded in an associative Coulomb soil. Int. J. Numer. Anal. Methods Geomech. 22 (11), 855–865.

Terzaghi, K., 1936. Stress distribution in dry and saturated sand above a yielding trapdoor. In: Proceedings of the 1st International Conference on Soil Mechanics and Foundation Engineering. Cambridge, Mass.

Terzaghi, K., 1943. Theoretical Soil Mechanics. Wiley Publishing, New York, USA.

Terzaghi, K., 1946. Rock Defects and Loads on Tunnel Supports. John Wiley and SonsInc.

Vardoulakis, I., Graf, B., Gudehus, G., 1981. Trap-door problem with dry sand: a statical approach based upon model test kinematics. Int. J. Numer. Anal. Methods Geomech 5 (1), 57–78.

Vesic, A.S., 1971. Breakout resistance of objects embedded in ocean bottom. In: Journal of the Soil Mechanics and Foundations Division, 97. ASCE, pp. 1183–1205 No. SM 9.

Wang, L., Leshchinsky, B., Evans, T.M., Xie, Y., 2017. Active and passive arching stress in C'-U' soils: a sensitivity study using computational limit analysis. Comput. Geotech. 84, 47–55.

Yodsomjai, W., Keawsawasvong, S., Lai, V.Q., 2021. Limit analysis solutions for bearing capacity of ring foundations on rocks using Hoek-Brown failure criterion. Int. J. Geosynth. Ground Eng. 7, 29.

Yodsomjai, W., Keawsawasvong, S., Likitlersuang, S., 2021. Stability of unsupported conical slopes in Hoek-Brown rock masses. Transp. Infrastruct. Geotechnol. 8, 278–295.